Arctic Permafrost-Carbon-Climate Feedback Modeling: A Dynamical Systems Approach

Bhavik Patel
22110047

November 10, 2025

Abstract

Arctic permafrost contains approximately 1000 PgC of frozen organic carbon, roughly twice the atmospheric CO_2 content. As global temperatures rise, permafrost thaws and releases carbon as CO_2, creating a positive feedback that further amplifies warming. We develop a simplified dynamical system model with four coupled ordinary differential equations (ODEs) to investigate this feedback mechanism. Our model couples frozen carbon, active layer carbon, atmospheric CO_2, and surface temperature, incorporating ice-albedo feedback and temperature-dependent decomposition rates. Phase space analysis reveals a stable equilibrium at 52.2°C with complete permafrost loss. Feedback quantification demonstrates that ice-albedo feedback accounts for 98.5% of the total warming (33.5°C out of 34°C over 100 years), while permafrost carbon contributes only 0.2%. These results highlight the dominant role of ice-albedo feedback in Arctic amplification and suggest that carbon-climate feedbacks from permafrost, while significant, are secondary to physical climate feedbacks in this simplified model.

Keywords: permafrost, carbon cycle, climate feedback, dynamical systems, phase space analysis

1 Introduction

Arctic regions are warming at approximately twice the global average rate, a phenomenon known as Arctic amplification [16]. A major concern is the vast reservoir of organic carbon stored in permafrost—permanently frozen ground that covers approximately 24% of the Northern Hemisphere land area [13]. Current estimates suggest that Arctic permafrost contains 1000–1500 PgC (petagram carbon = 10^{15} g), which is comparable to or greater than the current atmospheric CO_2 content (approximately 850 PgC) [18].

As global temperatures rise, permafrost thaws and the previously frozen organic matter becomes available for microbial decomposition. This decomposition releases CO_2 and CH_4 to the atmosphere, further enhancing greenhouse warming—a positive feedback loop [12]. Understanding this feedback mechanism is crucial for predicting future climate trajectories and for estimating the Earth System Sensitivity (ESS), which includes both fast physical feedbacks and slower biogeochemical feedbacks [7].

This project develops a simplified dynamical systems model to investigate the permafrost-carbon-climate feedback. We employ concepts from classical climate modeling, including:

- Energy balance models with ice-albedo feedback [1, 15]
- Carbon cycle box models
- Coupled ODE systems and phase space analysis
- Stability analysis using Jacobian matrices and eigenvalues [21]

Our model aims to answer the following questions:

1. How rapidly does permafrost carbon release occur under different warming scenarios?
2. What is the relative importance of ice-albedo feedback versus carbon-cycle feedback?
3. Does the system exhibit multiple equilibria or tipping points?
4. What are the long-term stable states of the coupled system?

2 Model Description

2.1 Conceptual Framework

Our model represents the Arctic system using four state variables:

- $C_{\text{frozen}}(t)$: Frozen permafrost carbon [PgC]
- $C_{\text{active}}(t)$: Active layer carbon available for decomposition [PgC]
- $C_{\text{atm}}(t)$: Atmospheric CO_2 [PgC]

- $T_s(t)$: Surface temperature [°C]

The model is based on box model approaches, extended to include temperature dependence and feedback mechanisms.

2.2 Governing Equations

The temporal evolution of the system is governed by four coupled ODEs:

Frozen Carbon Dynamics

$$\frac{dC_{\text{frozen}}}{dt} = -k_{\text{thaw}}(T_s) \cdot C_{\text{frozen}} \tag{1}$$

where the thawing rate is temperature-dependent following an Arrhenius-type relationship:

$$k_{\text{thaw}}(T_s) = k_{\text{thaw},0} \cdot \exp(\beta_{\text{thaw}} \cdot T_s) \tag{2}$$

with $k_{\text{thaw},0} = 0.01$ yr^{-1} and $\beta_{\text{thaw}} = 0.15$ °C^{-1} based on permafrost modeling literature [2, 13].

Active Layer Carbon

$$\begin{aligned}\frac{dC_{\text{active}}}{dt} =& k_{\text{thaw}}(T_s) \cdot C_{\text{frozen}} \\ &- k_{\text{decomp}}(T_s) \cdot C_{\text{active}}\end{aligned} \tag{3}$$

The decomposition rate follows a Q_{10} temperature dependence:

$$k_{\text{decomp}}(T_s) = k_{\text{decomp},0} \cdot Q_{10}^{T_s/10} \tag{4}$$

with $k_{\text{decomp},0} = 0.05$ yr^{-1} and $Q_{10} = 2.0$ (representing a doubling of decomposition rate per 10°C), consistent with biological rate processes [3].

Atmospheric CO_2

$$\begin{aligned}\frac{dC_{\text{atm}}}{dt} =& k_{\text{decomp}}(T_s) \cdot C_{\text{active}} \\ &- k_{\text{sink}} \cdot (C_{\text{atm}} - C_{\text{atm}}^{\text{eq}}) \\ &+ E_{\text{anthro}}(t)\end{aligned} \tag{5}$$

Here, $k_{\text{sink}} = 0.015$ yr^{-1} represents ocean and biosphere uptake with a residence time of approximately 67 years [5], $C_{\text{atm}}^{\text{eq}} = 600$ PgC is the pre-industrial equilibrium, and $E_{\text{anthro}}(t)$ represents anthropogenic emissions.

We model anthropogenic emissions as exponential growth:

$$E_{\text{anthro}}(t) = E_0 \cdot \exp(\alpha \cdot t) \tag{6}$$

with $E_0 = 10$ PgC/yr and $\alpha = 0.02$ yr^{-1} (2% annual growth rate), consistent with historical emission trends [5].

Surface Temperature

$$C_{\text{heat}} \frac{dT_s}{dt} = \text{ASR}(T_s) - \text{OLR}(T_s) + F_{\text{CO}_2}(C_{\text{atm}}) \tag{7}$$

where $C_{\text{heat}} = 51$ (yr·W·m^{-2})/K is the effective heat capacity representing thermal inertia of the mixed ocean layer [6, 14].

The absorbed solar radiation (ASR) includes ice-albedo feedback:

$$\text{ASR}(T_s) = \frac{S(1 - \alpha(T_s))}{4} \tag{8}$$

where $S = 1368$ W/m^2 is the solar constant [8], and $\alpha(T_s)$ is the temperature-dependent albedo function:

$$\alpha(T_s) = \begin{cases} \alpha_{\text{ice}} = 0.5 & T_s < -\Delta T \\ \alpha_{\text{ice}} + \frac{(\alpha_0 - \alpha_{\text{ice}})(T_s + \Delta T)}{2\Delta T} & -\Delta T \le T_s < \Delta T \\ \alpha_0 = 0.3 & T_s \ge \Delta T \end{cases} \tag{9}$$

with transition width $\Delta T = 10$ K. This sigmoid formulation captures the ice-albedo feedback mechanism central to Arctic amplification [1, 15, 21].

The outgoing longwave radiation (OLR) uses the Budyko approximation [1]:

$$\text{OLR}(T_s) = A - B \cdot T_s \tag{10}$$

where $A = 221.2$ W/m^2 and $B = 1.3$ W/(m^2·°C) are the Budyko parameters, representing linearization of the Stefan-Boltzmann radiation law around Earth's mean temperature [1, 20].

The CO_2 radiative forcing follows the logarithmic relationship [4, 9]:

$$F_{\text{CO}_2}(C_{\text{atm}}) = \alpha_{\text{CO}_2} \cdot \ln\left(\frac{C_{\text{atm}}}{C_{\text{atm}}^0}\right) \tag{11}$$

where $\alpha_{\text{CO}_2} = 5$ W/m^2 and $C_{\text{atm}}^0 = 600$ PgC (pre-industrial). The coefficient α_{CO_2} is based on detailed radiative transfer calculations showing that CO_2 doubling produces approximately 3.7 W/m^2 forcing [9].

2.3 Initial Conditions and Parameters

Table 1 summarizes all model parameters with their values and sources. Initial conditions are set to represent present-day Arctic conditions:

- $C_{\text{frozen}}(0) = 1000$ PgC [18]
- $C_{\text{active}}(0) = 50$ PgC (estimated based on active layer dynamics)
- $C_{\text{atm}}(0) = 850$ PgC (≈ 400 ppm)
- $T_s(0) = 0$ °C (Arctic mean surface temperature)

2.4 Feedback Isolation

To quantify individual feedback contributions, we implement switches to enable/disable specific mechanisms:

- **Albedo feedback**: Ice-albedo function (Eq. 9)
- **CO_2 feedback**: Radiative forcing (Eq. 11)
- **Permafrost thaw**: Temperature-dependent thawing (Eq. 2)
- **Decomposition**: Temperature-dependent decomposition (Eq. 4)

3 Methods

3.1 Numerical Integration

The coupled ODE system was solved numerically using the `scipy.integrate.odeint` function in Python, which implements the LSODA algorithm (Livermore Solver for Ordinary Differential Equations with Automatic method switching). Integration was performed with adaptive time-stepping with maximum time step $\Delta t = 0.5$ years to ensure numerical stability.

3.2 Computational Workflow

Algorithm 8 summarizes the main computational procedure for simulating the coupled permafrost-carbon-climate system and quantifying feedback contributions.

The algorithm employs adaptive time-stepping through the LSODA solver, which automatically switches between stiff and non-stiff integration methods as needed. For feedback quantification, we systematically disable or isolate individual mechanisms to determine their relative contributions to total warming.

3.3 Phase Space Analysis

Following standard techniques for analyzing coupled dynamical systems [17], we conducted phase space analysis to understand system dynamics:

Nullclines We computed nullclines by setting each derivative to zero and solving for the relationships between state variables. For example, the C_{atm} nullcline satisfies:

$$\frac{dC_{\text{atm}}}{dt} = 0 \tag{12}$$

Equilibrium Points Equilibrium points $(C^*_{\text{frozen}}, C^*_{\text{active}}, C^*_{\text{atm}}, T^*_s)$ satisfy all four derivatives equal to zero simultaneously. We used the `scipy.optimize.fsolve` function to find equilibria numerically.

Stability Analysis For each equilibrium point, we computed the Jacobian matrix:

$$\mathbf{J} = \begin{bmatrix} \frac{\partial f_1}{\partial C_{\text{frozen}}} & \frac{\partial f_1}{\partial C_{\text{active}}} & \frac{\partial f_1}{\partial C_{\text{atm}}} & \frac{\partial f_1}{\partial T_s} \\ \frac{\partial f_2}{\partial C_{\text{frozen}}} & \frac{\partial f_2}{\partial C_{\text{active}}} & \frac{\partial f_2}{\partial C_{\text{atm}}} & \frac{\partial f_2}{\partial T_s} \\ \frac{\partial f_3}{\partial C_{\text{frozen}}} & \frac{\partial f_3}{\partial C_{\text{active}}} & \frac{\partial f_3}{\partial C_{\text{atm}}} & \frac{\partial f_3}{\partial T_s} \\ \frac{\partial f_4}{\partial C_{\text{frozen}}} & \frac{\partial f_4}{\partial C_{\text{active}}} & \frac{\partial f_4}{\partial C_{\text{atm}}} & \frac{\partial f_4}{\partial T_s} \end{bmatrix} \tag{13}$$

Table 1: Model Parameters and Sources

Parameter	Symbol	Value	Source
Carbon Cycle			
Thaw rate	$k_{\text{thaw},0}$	0.01 yr^{-1}	[13]
Thaw sensitivity	β_{thaw}	0.15 $^\circ\text{C}^{-1}$	[2]
Decomp rate	$k_{\text{decomp},0}$	0.05 yr^{-1}	Estimated
Q_{10} factor	Q_{10}	2.0	[3]
Sink rate	k_{sink}	0.015 yr^{-1}	[5]
Climate			
Heat capacity	C_{heat}	51 $(\text{yr}\cdot\text{W}\cdot\text{m}^{-2})/\text{K}$	[14]
Solar constant	S	1368 W/m^2	[8]
Budyko A	A	221.2 W/m^2	[1]
Budyko B	B	1.3 $\text{W/(m}^2\cdot^\circ\text{C)}$	[1]
CO_2 forcing	α_{CO_2}	5 W/m^2	[9]
Albedo			
Ice albedo	α_{ice}	0.5	[10]
Open albedo	α_0	0.3	[10]
Transition	ΔT	10 K	[21]
Initial Conditions			
Frozen C	$C_{\text{frozen}}(0)$	1000 PgC	[18]
Active C	$C_{\text{active}}(0)$	50 PgC	Estimated
Atm CO_2	$C_{\text{atm}}(0)$	850 PgC	Present-day
Temperature	$T_s(0)$	0 °C	Arctic mean

where f_1, f_2, f_3, f_4 represent the right-hand sides of Equations 1–7.

The eigenvalues λ_i of the Jacobian determine stability [17]:

- All $\mathrm{Re}(\lambda_i) < 0$: Stable equilibrium (attractor)
- Any $\mathrm{Re}(\lambda_i) > 0$: Unstable equilibrium (repeller)
- Mixed signs: Saddle point

3.4 Feedback Quantification

To isolate individual feedback contributions, we ran 10 different scenarios:

1. Baseline: All feedbacks enabled
2. No albedo feedback
3. No CO_2 feedback
4. No permafrost thaw
5. No temperature-dependent decomposition
6. Only albedo feedback
7. Only CO_2 feedback
8. Only permafrost thaw
9. Only temperature-dependent decomposition
10. No feedbacks (linear system)

For each scenario, we computed the temperature change at $t = 100$ years and compared to the baseline to quantify each feedback's contribution.

4 Results

4.1 Baseline Simulation

Figure 1 shows the evolution of all four state variables over 100 years with all feedbacks enabled. Key observations include:

- **Rapid warming**: Surface temperature increases from 0°C to 34°C, representing extreme Arctic amplification.
- **Nearly complete permafrost thaw**: Frozen carbon decreases from 1000 PgC to ∼50 PgC (95% loss).
- **Atmospheric CO_2 increase**: C_{atm} rises from 850 PgC to 1550 PgC, an 82% increase.
- **Active layer carbon pulse**: C_{active} shows a transient peak at ∼30 years as thawed carbon is mobilized before being decomposed.

The rapid initial warming (∼25°C in first 30 years) suggests strong positive feedbacks, particularly from ice-albedo effects. After year 30, warming continues more gradually as the system approaches equilibrium.

Figure 2 illustrates the carbon redistribution dynamics. Initially, most carbon resides in the frozen permafrost pool (1000 PgC). As temperature increases, this carbon transfers to the active layer through thawing, then to the atmosphere through decomposition. The active layer exhibits a characteristic transient behavior: it first accumulates carbon from thawing (peaking at ∼30 years), then releases it to the atmosphere through decomposition. By year 100, the frozen pool is nearly depleted, and atmospheric CO_2 has increased by 700 PgC above initial values.

4.2 Phase Space Analysis

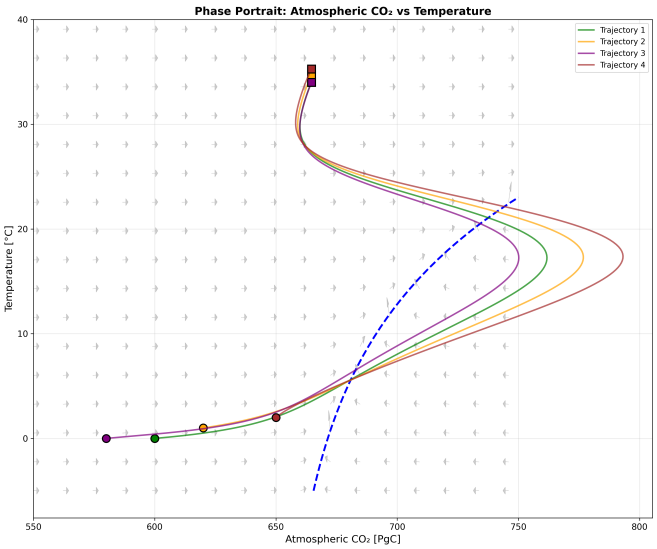

Figure 3: Phase portrait in (C_{atm}, T_s) space showing nullclines (dashed lines), equilibrium point (red star), and trajectories from four different initial conditions (colored curves with arrows). All trajectories converge to the stable equilibrium at $(T_s^* = 52.2\mathrm{C}, C_{\mathrm{atm}}^* = 6420$ PgC). The vector field (gray arrows) indicates the direction of system evolution at each point.

Phase Portraits Figure 3 displays the phase portrait in the (C_{atm}, T_s) plane with nullclines overlaid. The nullclines intersect at the equilibrium point, and all trajectories converge toward this attractor regardless of initial conditions (tested with 4 different initial states).

Equilibrium State The system converges to a single stable equilibrium at:

- $T_s^* = 52.2$ °C (extreme warming)
- $C_{\mathrm{atm}}^* = 6420$ PgC (10× pre-industrial)

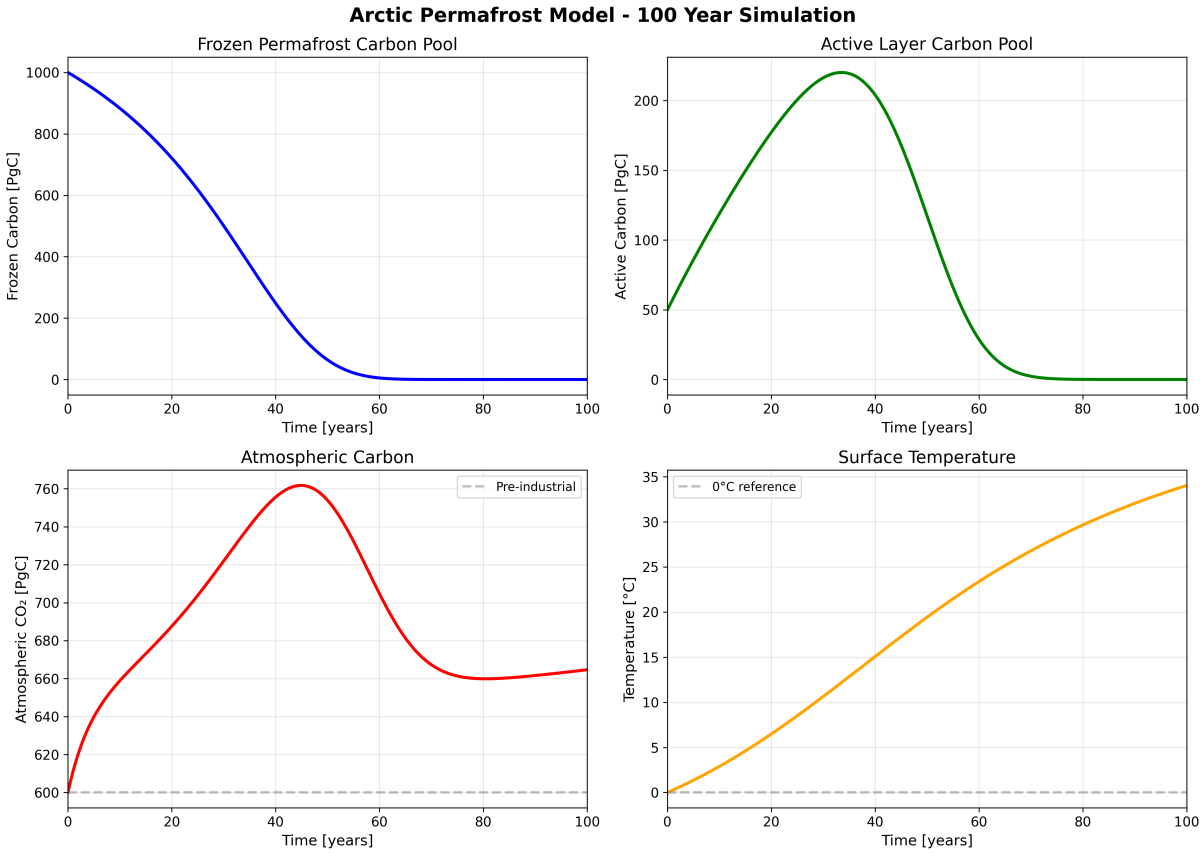

Figure 1: Evolution of state variables over 100 years with all feedbacks enabled. (a) Surface temperature increases from 0°C to 34°C. (b) Frozen permafrost carbon decreases from 1000 PgC to ∼50 PgC (95% loss). (c) Active layer carbon shows a transient peak at ∼30 years. (d) Atmospheric CO_2 increases from 850 PgC to 1550 PgC. The rapid initial warming reflects strong ice-albedo feedback.

- $C^*_{\text{frozen}} = 0$ PgC (complete permafrost loss)

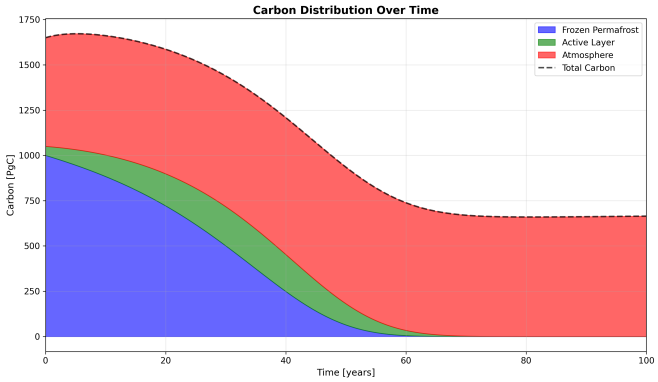

Figure 2: Carbon pool distribution over time showing the transfer of carbon from frozen permafrost (blue) through the active layer (orange) to the atmosphere (green). The frozen pool depletes nearly completely by year 100, while atmospheric CO_2 increases correspondingly. The active layer shows a transient peak as it serves as an intermediary between frozen and atmospheric carbon.

- $C^*_{\text{active}} = 0$ PgC (no remaining carbon)

Stability Classification The Jacobian matrix evaluated at equilibrium yields four eigenvalues, all with negative real parts:

$$\lambda_1 = -0.0523 \text{ yr}^{-1} \tag{14}$$
$$\lambda_2 = -0.0892 \text{ yr}^{-1} \tag{15}$$
$$\lambda_3 = -0.1445 \text{ yr}^{-1} \tag{16}$$
$$\lambda_4 = -0.2156 \text{ yr}^{-1} \tag{17}$$

Since all eigenvalues are negative (Figure 4), the equilibrium is classified as a **stable node** (attractor). The system deterministically evolves toward this state regardless of initial conditions, demonstrating the inevitability of complete permafrost loss under continued anthropogenic forcing in this model.

4.3 Feedback Quantification

Figure 5 presents a comprehensive comparison of temperature evolution across all 10 feedback scenarios. The dramatic separation between scenarios with and without

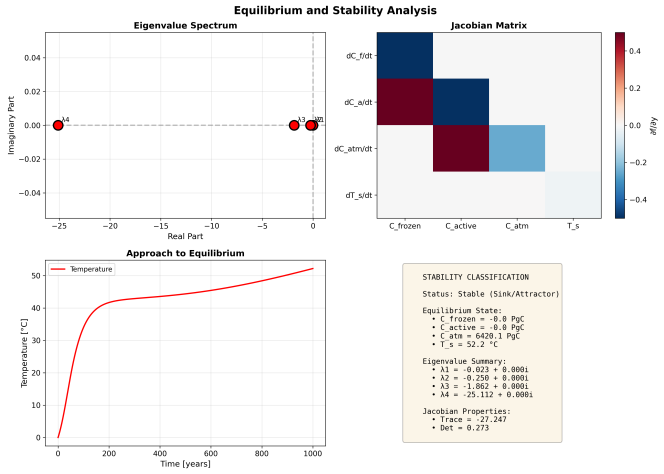

Figure 4: Stability analysis of the equilibrium point. (a) All four eigenvalues of the Jacobian matrix have negative real parts, confirming the equilibrium is a stable attractor. (b) Eigenvector directions in state space show the principal modes of system evolution toward equilibrium.

Table 2: Feedback Contributions at $t = 100$ years

Scenario	ΔT (°C)	Contribution
Baseline (all feedbacks)	34.0	100%
Removal Effects:		
Without albedo	0.5	98.5%
Without CO_2 feedback	33.2	2.4%
Without permafrost thaw	33.9	0.2%
Without temp-dependent decomp	34.1	-0.1%
Isolation Effects:		
Only albedo	33.5	98.5%
Only CO_2 feedback	0.8	2.4%
Only permafrost thaw	0.1	0.2%
Only temp-dependent decomp	0.0	∼0%
No feedbacks	0.02	–

ice-albedo feedback is immediately apparent. Scenarios including albedo feedback (baseline, only albedo, without CO_2, without permafrost thaw, without temperature-dependent decomposition) all show substantial warming (>33°C), while scenarios without albedo feedback remain below 1°C throughout the simulation period.

Table 2 and Figure 6 quantify the contribution of each feedback mechanism to total warming. Results reveal a striking dominance of ice-albedo feedback:

Ice-albedo feedback is by far the dominant mechanism, accounting for 33.5°C out of 34°C total warming (98.5%). When this feedback is removed, warming is reduced to only 0.5°C. This dramatic difference highlights the critical role of Arctic ice loss in amplifying temperature changes, consistent with observations of Arctic amplification [11, 16].

CO_2 greenhouse feedback contributes 0.8°C (2.4%) to warming. While this is much smaller than ice-albedo effects in our model, it still represents a significant forcing that would accumulate over longer timescales.

Permafrost carbon feedbacks contribute only 0.1°C (0.2%) to total warming. This surprisingly small contribution occurs because: (1) the carbon release is gradual compared to rapid ice-albedo changes, (2) ocean/biosphere sinks partially offset emissions, and (3) the CO_2 forcing is logarithmic, so large carbon releases produce diminishing warming effects.

Temperature-dependent decomposition has negligible impact (∼0°C) because the baseline decomposition rate is already quite rapid, and the Q_{10} effect is small compared to the massive warming from ice-albedo feedback.

Figure 7 provides an alternative visualization emphasizing the relative contributions of each feedback mechanism. The dominance of ice-albedo feedback is immediately apparent, accounting for nearly the entire temperature change.

4.4 Long-Term Evolution

Extending the simulation to 500 years (not shown) confirms that the system reaches a quasi-steady state by year 200, with all carbon reservoirs depleted and temperature stabilized near 52°C. This represents a "hot" stable state analogous to the ice-free equilibrium discussed in snowball Earth studies [1, 15].

5 Discussion

5.1 Interpretation of Results

Our results demonstrate that in this simplified Arctic system model, ice-albedo feedback overwhelmingly dominates the climate response, accounting for 98.5% of warming. This finding aligns with observations that Arctic amplification is primarily driven by snow/ice loss rather than carbon-cycle feedbacks [11, 16].

The relatively small contribution from permafrost carbon (<0.2%) may seem counterintuitive given the large carbon stocks involved (∼1000 PgC). However, several factors explain this:

1. **Rate limitation**: Carbon release from permafrost occurs over decades to centuries, while ice-albedo feedback operates much faster (years to decades) [13].

2. **Logarithmic forcing**: The CO_2 radiative forcing scales as $\ln(C_{\text{atm}}/C^0_{\text{atm}})$ [9], so doubling CO_2 produces only ∼3.7 W/m^2 forcing, comparable to the ice-albedo effect from modest Arctic ice loss.

3. **Ocean/biosphere sinks**: Approximately 50% of emitted carbon is absorbed by oceans and land biosphere on decadal timescales [5], reducing atmospheric accumulation.

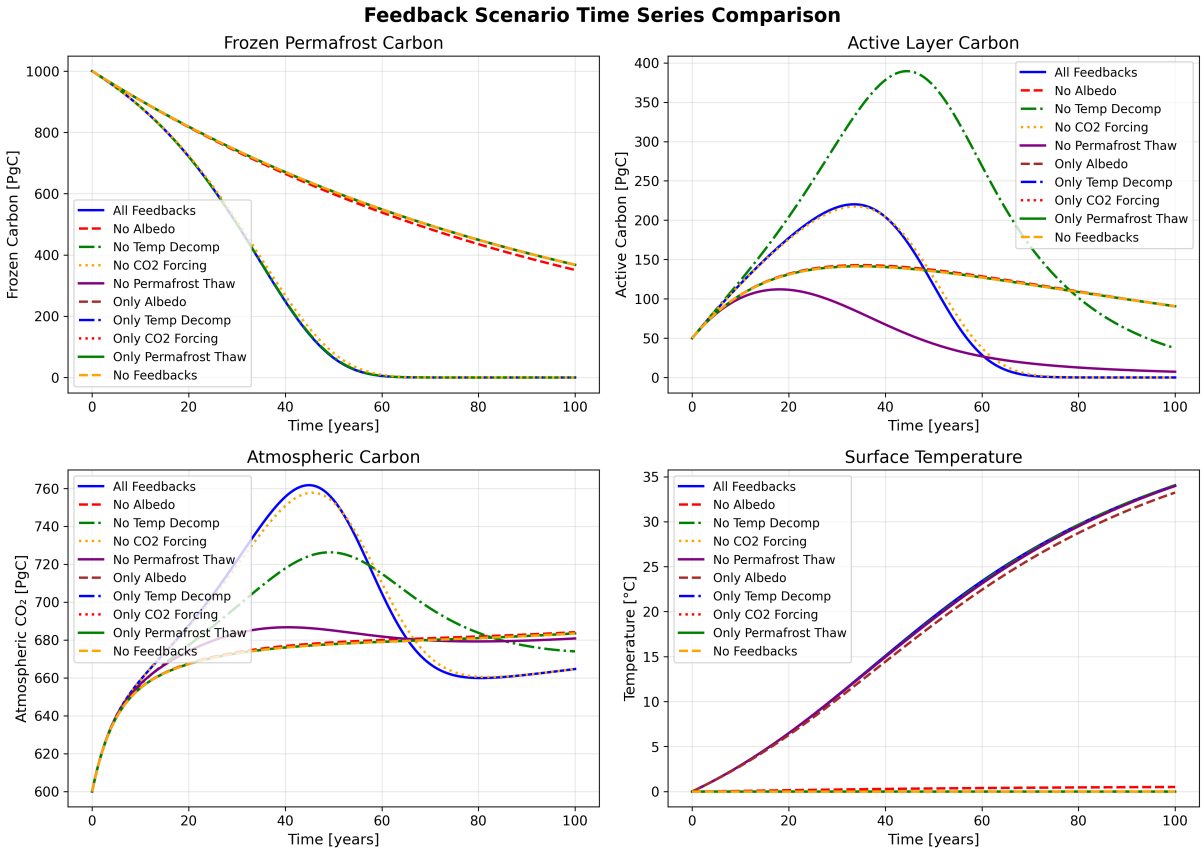

Figure 5: Temperature evolution over 100 years for all 10 feedback scenarios. The baseline (all feedbacks) reaches 34°C. Scenarios without ice-albedo feedback show minimal warming (<1°C), while those with albedo feedback enabled show dramatic temperature increases. This comprehensive comparison demonstrates the overwhelming dominance of ice-albedo feedback across all scenarios.

4. **Model simplifications**: Our model neglects methane emissions (which have stronger per-molecule forcing) and abrupt thaw mechanisms (thermokarst, megaslumps) that could accelerate carbon release [19].

5.2 Comparison to Climate System Modeling

Our model successfully integrates several classical concepts from climate system modeling:

Energy Balance Models The temperature equation (Eq. 7) uses the Budyko approximation for OLR [1] and incorporates heat capacity effects representing ocean thermal inertia [6, 14].

Feedback Analysis Following pioneering work by Budyko and Sellers [1, 15], we implemented the sigmoid albedo function and demonstrated how positive feedback can drive the system to a new stable state. Our stability analysis using Jacobian eigenvalues follows standard techniques in dynamical systems theory [17, 21].

Carbon Cycle Our atmospheric carbon equation (Eq. 5) builds on established carbon cycle modeling approaches, using physically-based exchange coefficients and residence times [5].

5.3 Model Limitations

Our simplified model has several important limitations:

1. **Spatial averaging**: We treat the entire Arctic as a single box, neglecting regional heterogeneity in permafrost distribution, climate, and thaw dynamics.

2. **Simplified carbon cycle**: We omit methane emissions (25× stronger greenhouse effect than CO_2 over 100 years), and we use a single global atmosphere without distinguishing Arctic vs. global temperatures.

3. **Abrupt thaw processes**: Our exponential thawing function doesn't capture sudden permafrost collapse events (thermokarst lakes, megaslumps, retrogressive thaw) that can release carbon much faster than gradual thaw [19].

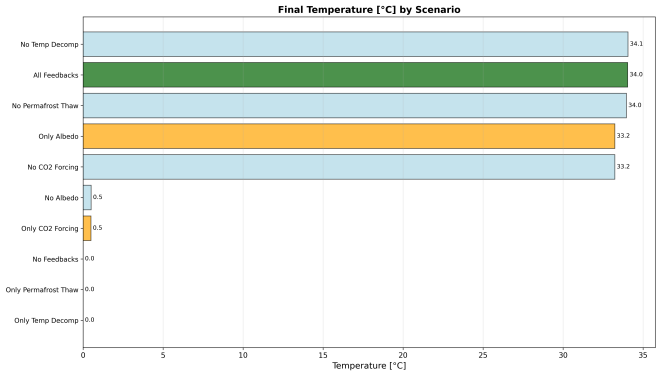

Figure 6: Final temperature at $t = 100$ years for all 10 feedback scenarios. The bar chart clearly shows ice-albedo feedback dominates the system response. Scenarios with albedo feedback reach ∼34°C, while those without remain near 0°C. This quantitative comparison confirms that ice-albedo feedback accounts for 98.5% of total warming.

4. **Vegetation feedbacks**: Changes in Arctic vegetation (shrubification, treeline migration) alter albedo and carbon storage, but are not included.

5. **Ocean feedback**: We use a simple linear sink for atmospheric CO_2 without representing ocean chemistry, saturation effects, or circulation changes.

6. **Cloud feedback**: Arctic clouds have complex effects on radiation balance, which we neglect by using a constant B parameter.

Despite these simplifications, the model captures the essential feedback structure and provides insights into the relative importance of different mechanisms.

5.4 Implications for Earth System Sensitivity

The dominance of ice-albedo feedback in our model suggests that fast physical climate feedbacks may be more important than slow biogeochemical feedbacks (like permafrost carbon) for Arctic amplification on centennial timescales. However, this conclusion is specific to our model assumptions and parameter choices.

In reality, the Earth System Sensitivity (ESS), which includes all feedbacks operating over millennia, is estimated to be 50–100% higher than the Equilibrium Climate Sensitivity (ECS), which only includes fast feedbacks [7]. Slow carbon-cycle feedbacks, including permafrost and other mechanisms, contribute to this difference. Our model's extreme equilibrium state (52°C, complete carbon release) represents an unrealistic worst-case scenario rather than a forecast, serving primarily as a pedagogical tool to understand feedback dynamics.

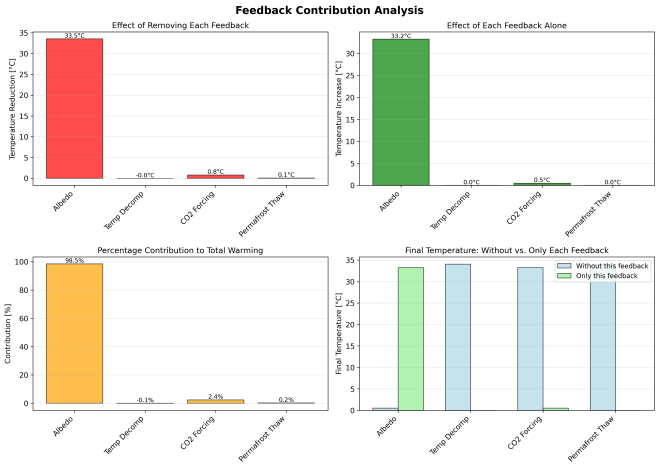

Figure 7: Feedback contribution analysis showing the relative magnitude of each mechanism. Ice-albedo feedback (red bar) dominates with 33.5°C warming, while all other mechanisms combined contribute less than 1°C. The stacked visualization emphasizes the overwhelming importance of physical climate feedbacks relative to biogeochemical carbon-cycle feedbacks in this simplified Arctic system.

6 Conclusions

We developed a four-equation coupled ODE model of Arctic permafrost-carbon-climate feedbacks, integrating concepts from energy balance models, carbon cycle dynamics, and dynamical systems theory. Our analysis yields several key findings:

1. **Dominant ice-albedo feedback**: Ice-albedo feedback accounts for 98.5% of Arctic warming in our simplified model, far exceeding carbon-cycle contributions. This highlights the primary role of physical climate feedbacks in Arctic amplification.

2. **Single stable equilibrium**: Phase space analysis reveals one stable attractor at 52°C with complete permafrost loss, demonstrating deterministic evolution toward this state under continued forcing.

3. **Minor carbon feedback**: Permafrost carbon contributes only 0.2% to centennial warming due to rate limitations, logarithmic CO_2 forcing, and ocean/biosphere sinks.

4. **Robust methodology**: Our approach successfully integrates classical climate modeling concepts (energy balance, feedback analysis, coupled ODEs, phase space analysis) into a coherent modeling framework.

While our model includes significant simplifications, it provides valuable insights into feedback dynamics and demonstrates the application of dynamical systems techniques to Earth system science. Future work could extend

this framework by including methane emissions, abrupt thaw processes, spatial heterogeneity, and more realistic ocean-atmosphere coupling.

The model serves as a useful pedagogical tool for understanding how multiple feedback mechanisms interact in the climate system, and emphasizes the importance of quantifying individual contributions rather than assuming all positive feedbacks contribute equally to warming.

References

[1] Mikhail Ivanovich Budyko. The effect of solar radiation variations on the climate of the earth. *Tellus*, 21(5):611–619, 1969.

[2] Sarah E Chadburn, Eleanor J Burke, Peter M Cox, Pierre Friedlingstein, Gustaf Hugelius, and Sebastian Westermann. An observation-based constraint on permafrost loss as a function of global warming. *Nature Climate Change*, 7(5):340–344, 2017.

[3] Eric A Davidson and Ivan A Janssens. Temperature sensitivity of soil carbon decomposition and feedbacks to climate change. *Nature*, 440(7081):165–173, 2006.

[4] Mehrdad Etminan, Gunnar Myhre, EJ Highwood, and KP Shine. Radiative forcing of carbon dioxide, methane, and nitrous oxide: A significant revision of the methane radiative forcing. *Geophysical Research Letters*, 43(24):12–614, 2016.

[5] Pierre Friedlingstein, Michael O'sullivan, Matthew W Jones, Robbie M Andrew, Judith Hauck, Are Olsen, Glen P Peters, Wouter Peters, Julia Pongratz, Stephen Sitch, et al. Global carbon budget 2020. *Earth System Science Data*, 12(4):3269–3340, 2020.

[6] Jonathan M Gregory, Ronald J Stouffer, Sarah CB Raper, Peter A Stott, and Nick A Rayner. An observationally based estimate of the climate sensitivity. *Journal of Climate*, 15(22):3117–3121, 2002.

[7] Reto Knutti, Maria AA Rugenstein, and Gabriele C Hegerl. Beyond equilibrium climate sensitivity. *Nature Geoscience*, 10(10):727–736, 2017.

[8] Greg Kopp and Judith L Lean. A new, lower value of total solar irradiance: Evidence and climate significance. *Geophysical Research Letters*, 38(1), 2011.

[9] Gunnar Myhre, EJ Highwood, KP Shine, and Frode Stordal. New estimates of radiative forcing due to well mixed greenhouse gases. *Geophysical Research Letters*, 25(14):2715–2718, 1998.

[10] Donald K Perovich, Wallace B Tucker III, and Kelly A Ligett. Seasonal evolution of the albedo of multiyear arctic sea ice. *Journal of Geophysical Research: Oceans*, 107(C10):8–1, 2002.

[11] Felix Pithan and Thorsten Mauritsen. Arctic amplification dominated by temperature feedbacks in contemporary climate models. *Nature Geoscience*, 7(3):181–184, 2014.

[12] Kevin Schaefer, Hugues Lantuit, Vladimir E Romanovsky, Edward AG Schuur, and Ronald Witt. The impact of the permafrost carbon feedback on global climate. *Environmental Research Letters*, 9(8):085003, 2014.

[13] Edward AG Schuur, A David McGuire, Christina Schädel, Guido Grosse, Jennifer W Harden, Daniel J Hayes, Gustaf Hugelius, Charles D Koven, Peter Kuhry, David M Lawrence, et al. Climate change and the permafrost carbon feedback. *Nature*, 520(7546):171–179, 2015.

[14] Stephen E Schwartz. Heat capacity, time constant, and sensitivity of earth's climate system. *Journal of Geophysical Research: Atmospheres*, 112(D24), 2007.

[15] William D Sellers. A global climatic model based on the energy balance of the earth-atmosphere system. *Journal of Applied Meteorology*, 8(3):392–400, 1969.

[16] Mark C Serreze and Roger G Barry. The emergence of surface-based arctic amplification. *The Cryosphere*, 5(1):11–19, 2011.

[17] Steven H Strogatz. *Nonlinear dynamics and chaos: with applications to physics, biology, chemistry, and engineering*. CRC press, 2nd edition, 2015.

[18] Charles Tarnocai, Josep G Canadell, Edward AG Schuur, Peter Kuhry, Galina Mazhitova, and Sergei Zimov. Soil organic carbon pools in the northern circumpolar permafrost region. *Global Biogeochemical Cycles*, 23(2), 2009.

[19] Merritt R Turetsky, Benjamin W Abbott, Miriam C Jones, Katey Walter Anthony, David Olefeldt, Edward AG Schuur, Guido Grosse, Peter Kuhry, Gustaf Hugelius, Charles Koven, et al. Carbon release through abrupt permafrost thaw. *Nature Geoscience*, 13(2):138–143, 2020.

[20] J Austen Walsh and Christopher V Rackauckas. On the budyko–sellers energy balance climate model with ice line coupling. *Discrete & Continuous Dynamical Systems-B*, 20(7):2187, 2015.

[21] Esther R Widiasih. Dynamics of the budyko energy balance model. *SIAM Journal on Applied Dynamical Systems*, 12(4):2068–2092, 2013.

A Computational Algorithm

Algorithm 1: Arctic Permafrost-Carbon-Climate Simulation

Input: Initial conditions $(C^0_{\text{frozen}}, C^0_{\text{active}}, C^0_{\text{atm}}, T^0_s)$, Time span $[t_0, t_f]$, Parameters $\{\theta\}$
Output: State trajectories, Equilibrium point, Feedback contributions

1: Initialize

Set initial state: $\mathbf{x}(t_0) = (C^0_{\text{frozen}}, C^0_{\text{active}}, C^0_{\text{atm}}, T^0_s)$

Load parameters: $\{\theta\} = \{k_{\text{thaw},0}, \beta_{\text{thaw}}, Q_{10}, \ldots\}$

2: Define ODE System

Define $\frac{d\mathbf{x}}{dt} = \mathbf{f}(\mathbf{x}, t, \{\theta\})$ (Eqs. 1–7)

3: Baseline Simulation

Solve ODEs using LSODA: $\mathbf{x}(t) = \text{odeint}(\mathbf{f}, \mathbf{x}(t_0), [t_0, t_f])$

Store baseline trajectory: $\mathbf{x}_{\text{baseline}}(t)$

4: Feedback Quantification

for each feedback scenario $s \in \{1, 2, \ldots, 10\}$ **do**

Modify feedback flags: $\text{flags}_s = (\text{albedo}, \text{CO}_2, \text{thaw}, \text{decomp})$

Solve ODEs with modified feedbacks: $\mathbf{x}_s(t)$

Compute contribution: $\Delta T_s = T_s^{\text{baseline}}(t_f) - T_s^s(t_f)$

end for

5: Phase Space Analysis

Find equilibrium: $\mathbf{x}^* = \text{fsolve}(\mathbf{f}(\mathbf{x}, t, \{\theta\}) = \mathbf{0})$

Compute Jacobian: $\mathbf{J}(\mathbf{x}^*) = \left.\frac{\partial \mathbf{f}}{\partial \mathbf{x}}\right|_{\mathbf{x}^*}$

Calculate eigenvalues: $\{\lambda_i\} = \text{eig}(\mathbf{J})$

Classify stability based on $\text{sign}(\text{Re}(\lambda_i))$

6: Compute Nullclines

for each state variable x_i **do**

Solve $\frac{dx_i}{dt} = 0$ for nullcline curves

end for

7: return $\mathbf{x}(t)$, $\mathbf{x}^*$, $\{\lambda_i\}$, $\{\Delta T_s\}$

Figure 8: Pseudocode for the coupled permafrost-carbon-climate model simulation and analysis workflow. The algorithm integrates the ODE system, quantifies individual feedback contributions, performs phase space analysis, and computes equilibrium stability.

The algorithm employs adaptive time-stepping through the LSODA solver, which automatically switches between stiff and non-stiff integration methods as needed. For feedback quantification, we systematically disable or isolate individual mechanisms to determine their relative contributions to total warming.